Steven Jenks

On Pole Trajectories of the S-Matrix for Various Attractive Potentials

In this paper, poles of the S-Matrix and their trajectory's are studied for various attractive potentials. It is shown that the trajectory of these poles change with the parameters of the potential, however the mathematical expressions describing these trajectories are fundamentally the same. First, the poles for a finite-depth square well potential, width L and depth V (V<0), are explored. The depth and width are then altered and the pole trajectories are compared. Lastly, the shape of the potential is changed to an attractive Gaussian and compared with the square well. It should be noted that Maple was used to produce the plots and most of the calculations throughout this paper. The appendix shows all the raw data and relevant Maple worksheets used to produce the various results.

Elements of the S-Matrix

A quick review of the S-Matrix reveals that the T-matrix element T_{11} appears in the denominator for each S-Matrix element. Therefore, the pole structure will be determined when $T_{11}=0$. The matrix element T_{11} is resolved by the boundary conditions (bound or scattering) as well as the various sizes and shapes of the attractive potential. It should be noted that the asymptotic left and right of all the various attractive potentials studied in this paper was constant at 0 eV.

Bound State Boundary Conditions (E<0)

As previously determined, when the energy is less then the asymptotic left and right the wave functions have the form;

$$\Psi_L=B_L e^{\kappa x}, \text{ with } \kappa=\text{sqrt}(2m(V_L-E)/\hbar^2)$$
$$\Psi_R=A_R e^{-\kappa x}, \text{ with } \kappa=\text{sqrt}(2m(V_R-E)/\hbar^2)$$
$$V_L=V_R=0$$

From these boundary conditions, the matrix element T_{11} can now be determined. The equation that is produced from the transfer matrix is $0=T_{11}*A_R$. In order to satisfy this equation the T_{11} has to equal 0 and our poles are found. It just so happens that these poles also correspond to the bound states inside the attractive potential. For the simple square well potential, the analytic equation shown below corresponds to T_{11}, and was found from the transfer matrix relating the asymptotic left with the right.

$$cos(k\cdot\delta)+\frac{1}{2}\cdot\left(\frac{\kappa}{k}-\frac{k}{\kappa}\right)\cdot sin(k\cdot\delta)$$

The values $k=(2*m*q(E-V)/\hbar^2)$ and $\kappa=\text{sqrt}(2*m*q*E/\hbar^2)$, where V corresponds the depth and δ to the width. The poles for various widths and depths were calculated (although not all are displayed here) and are shown below in the plots. When T_{11} crosses 0, a pole is found.

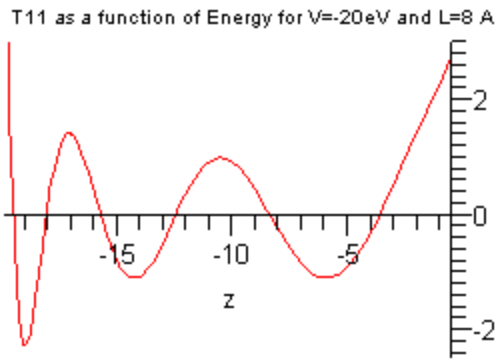

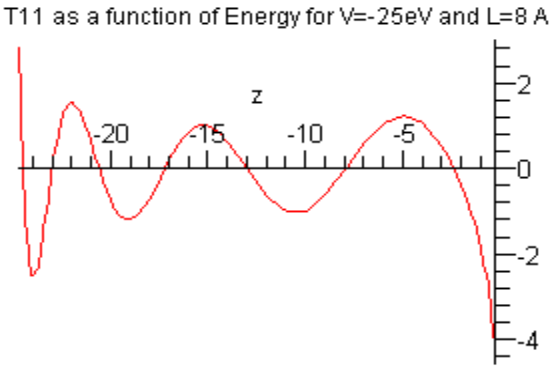

Figure 1 (left)-attracting potential where V= -20 eV and L=8 A. **Figure 2 (right)**-attracting potential where V= -25eV and L=8 A.

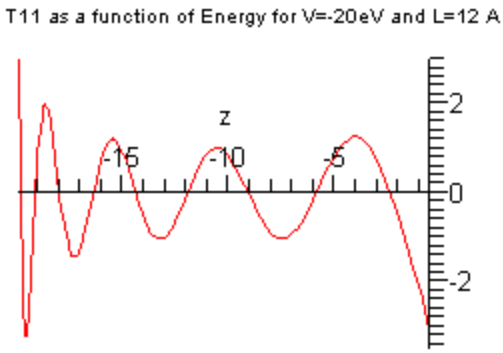

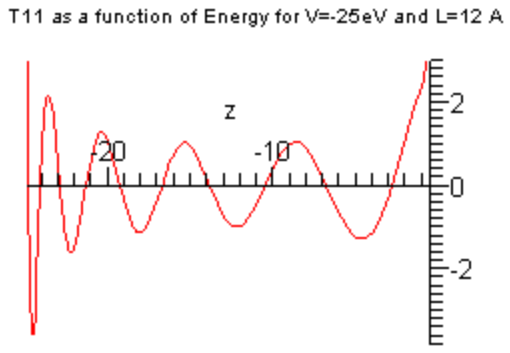

Figure 3 (left)-attracting potential where V= -20 eV and L=12 A. **Figure 4 (right)**-attracting potential where V= -25eV and L=12 A.

A quick observation shows that in figure 1 there are 6 poles, figure 2 there are 7 poles, figure 3 there are 9 poles, and in figure 4 there are 10 poles. The assumption that when the potential is deepened or the width is stretched, more bounds states/poles are present is correct and has been confirmed in *Elementary Quantum Mechanics in One Dimension*, by Gilmore. To address the pole trajectory question, it is seen that the poles shift on the real energy axis for the various depths and widths. These results are expected and a bit uninteresting.

Now let's take a look at an attractive Gaussian that has the form $V(x)=-V_0e^{-x\hat{}2}$ and locate the bound states. This potential was studied by making a piecewise approximation to it, specifically an 11-piecewise approximation. Unlike the attracting square well potential, an explicit expression for T_{11} cannot be generated, as it is calculated numerically. The code was written in Maple and included in the Appendix. The poles for the attracting Gaussian are shown below and as before when T_{11} crosses 0 a pole is found.

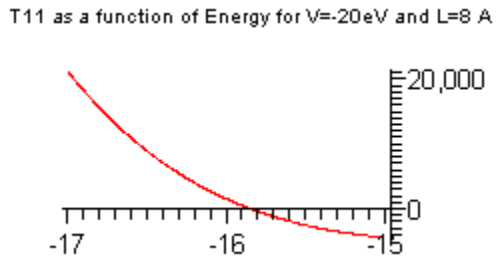

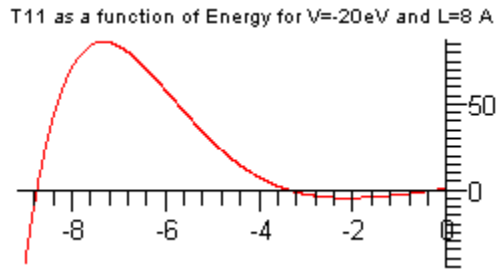

Figure 5 (left and right)-11-piece approximation for the attractive Gaussian potential where V_0= -20eV and L=8 A.

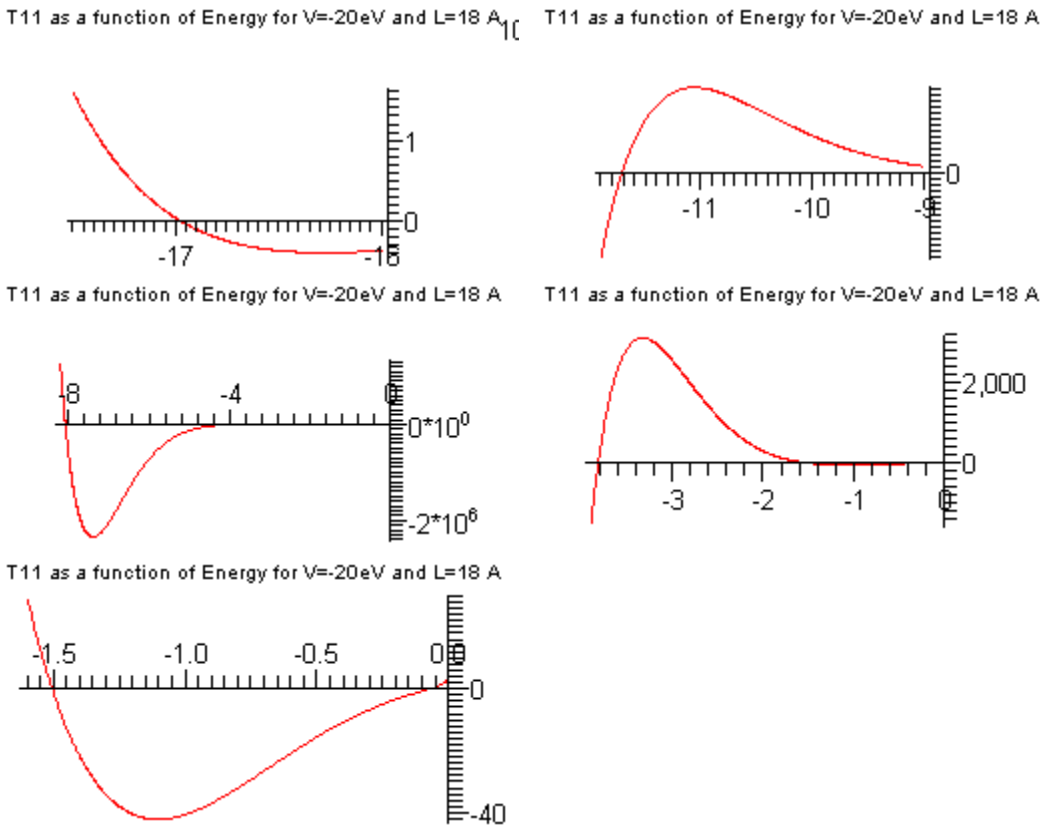

Figure 6-11-piece approximation for the attractive Gaussian potential where V_0= -20eV and L=18 A.

In figure 5 there are 4 poles and in figure 6 there are 6 poles. T_{11} is more extreme for the Gaussian potential as indicated by the two figures; however the poles still shift on the real energy axis for the various widths and one can assume that the same would happen if the depth was varied.

It has been explicitly shown that poles or bound states of potentials with varying parameters shift on the real energy axis. It is only logical to observe where the poles are and how the poles shift when scattering boundary conditions are satisfied. From the previous study, it was shown that there are poles in the complex energy plane and these poles shift when the parameters (width and height) of the potential change. What is the trajectory that these poles follow? Does this trajectory change and if it does how? These questions are now addressed.

Scattering boundary conditions (E>0)

When the particle is associated with an energy that is greater then the asymptotic left and right (in this case >0) scattering occurs. The boundary conditions for scattering are obviously different then the boundary conditions for bound states, therefore the matrix element T_{11} will change. If a particle is incident from the left the wavefunction is $A_L e^{+ikx}$ and the reflected wavefunction is $B_L e^{-ikx}$ with $k=\sqrt{2m(E-V_L)/\hbar^2}$, while the transmitted wavefunction is $A_R e^{+ikx}$ with $k=\sqrt{2m(E-V_R)/\hbar^2}$. The wavefunction for the particle that is incident from the right must be 0, therefore B_R vanishes[1]. The matrix element T_{11} can be determined from these boundary conditions and poles can be found. For a square-well potential T_{11} is an analytic function that has the form;

$$cos(kprime\cdot\ \delta) - \frac{i}{2}\left(\frac{kprime}{k} + \frac{k}{kprime}\right) sin(kprime\cdot\ \delta)$$

where, k'(kprime)=sqrt(2*m*(E-V)/$\hbar^2$), k=sqrt(2*m*E/ $\hbar^2$) and δ is the width. For the attractive Gaussian piecewise approximation, T_{11} is found through numerical calculations (codes written in Maple are found in the appendix).

Before studying the pole structure/trajectory for various potentials, the transmission probability and scattering resonances are first determined. Below are various plots of the transmission probability for the square-well with varying parameters and the piecewise approximation to the attractive Gaussian.

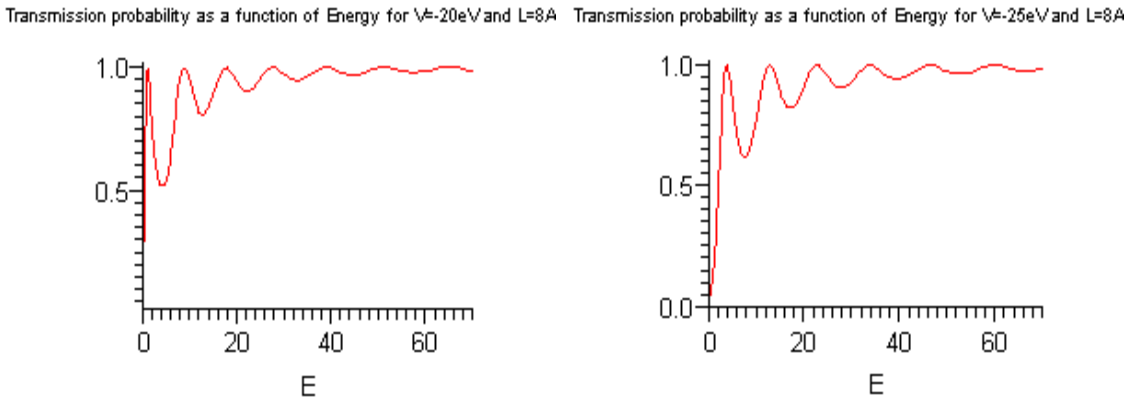

Figures 7 (Left) and 8(Right)-Transmission probability for square well potentials V=-20eV and -25eV, with δ=8A.

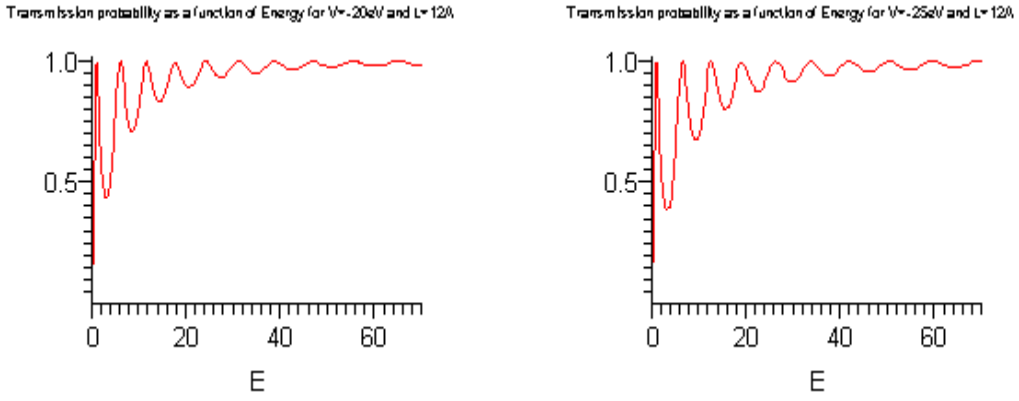

Figures 9 (Left) and 10 (Right)-Transmission probability for square well potentials V=-20eV and -25eV, with δ=12A.

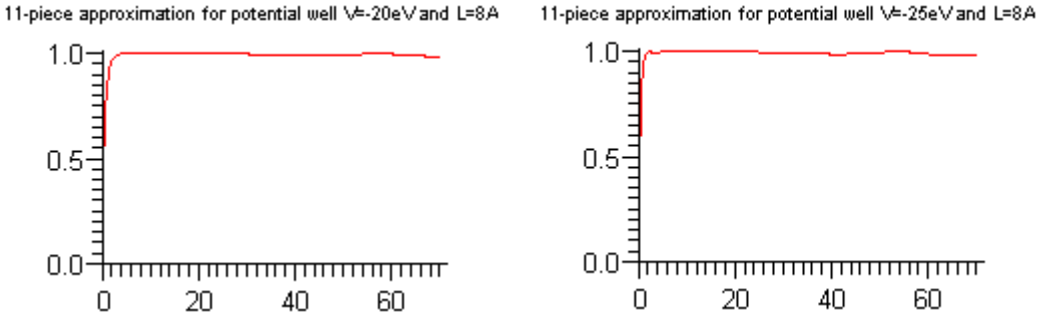

Figures 11 (Left) and 12(Right)-Transmission probability for attracting piecewise approximation for the Gaussian potential V=-20eV and -25eV, with δ=8A.

V=-20eV δ=8A	V=-20eV δ=12A	V=-25eV δ=8A	V=-25eV δ=12A
1.12966491	1.12966491	3.75982169	1.08600606
8.75982169	6.08600606	12.56384873	6.56406733
17.56384873	11.56406733	22.54174604	12.56384873
27.54174604	17.56384873	33.69351362	19.08535026
38.69351362	24.08535026	46.01915151	26.12857189
51.01915151	31.12857189	59.51865967	33.69351362
64.51865967	38.69351362	74.19203805	41.78017551
79.19203805	46.78017551	90.0392868	50.38855753

Table 1-scattering resonances for the square well potential with varying parameters.

Table 1 shows that as the potentials are widened there exists more resonances and as the potential is deepened the resonances shift on the real energy axis. Figures 11 and 12 show the transmission probability for an attractive Gaussian potential, these figures are very different from the square potential. The transmission probability is very close to 1 in both figures and the resonance structure that appeared in the square well appears to have disappeared. However upon closer inspection of the transmission probability, some resonance structure appears as seen below. Notice that the transmission probability varies from .98 to 1.0!

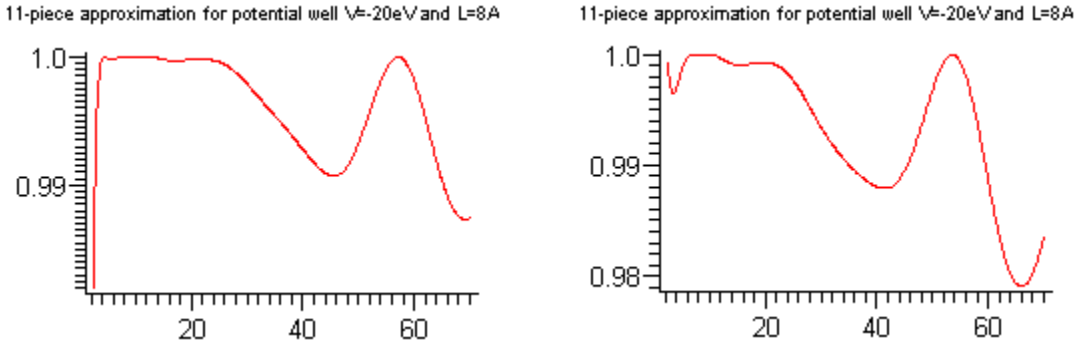

Figures 13 (left) and 14 (right) - Transmission probability for attracting piecewise approximation for the Gaussian potential V=-20eV and -25eV, with δ=8A starting with Energy >2.

To each resonance, there corresponds a simple pole of the S-Matrix in the complex energy plane[2]. In order to find these poles, we look to see where the matrix element T_{11} is 0 and plot this energy in the complex plane. Then a simple mathematical expression for this trajectory is found. Finding the poles for the square well potential is investigated first. It has been shown in my previous paper exactly how the poles are found for the square well potential, so for the purposes of this paper I refer the reader to *On the Pole Structure of the S-Matrix for a Square Well Potential.* Poles were found for various widths and depths, figure 15 shows the pole trajectories of varied depth and figure 16 shows the pole trajectories of varied width. It is seen that the trajectory of the curve is more susceptible to change from varying the width rather the depth. Also, as the depth of the well increases the poles shift to closer to the imaginary axis (see previous paper mentioned above) and some of these poles are transformed into bound states. This shift occurs as a whole, i.e. the distance between them do not change relative to one another. As the potential is widened, more poles appear.

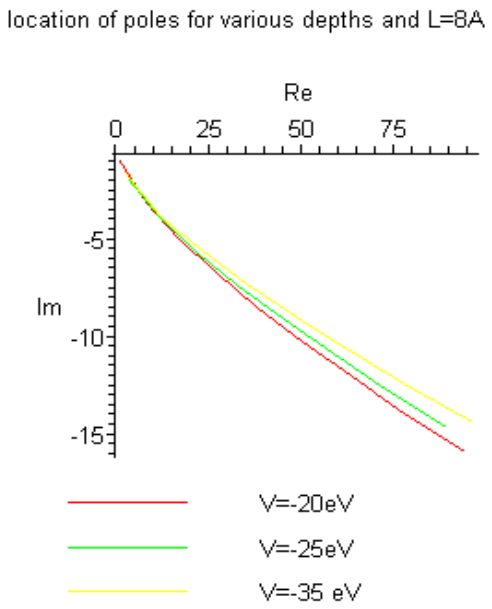

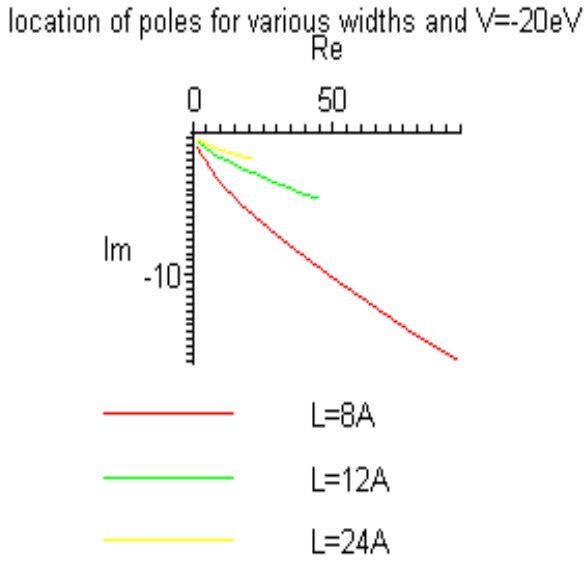

Figure 15 (top)-Poles on the complex energy plane for varying depths. **Figure 16 (bottom)-**Poles on the complex energy plane for varying widths. In order to emphasize the poles trajectory, a line plot was used instead of the discrete poles.

It is seen from above that when the parameters of the square well potential are varied, the trajectory of the poles shift. As the depth and width increase, the imaginary part of the energy decreases. Even though the trajectory changes, the mathematical expression describing it is the same and after some educated guesses the expression looks like the following;

$$Trajectory\ Curve = a\,z + b\sqrt{z}$$

with a and b being constant, while z is the real part of the energy (independent variable). It should also be noted that there is a vertical tangency at the origin, as expected. To show how good a fit this curve is to the pole trajectory, it is applied to various potentials with only a few shown below.

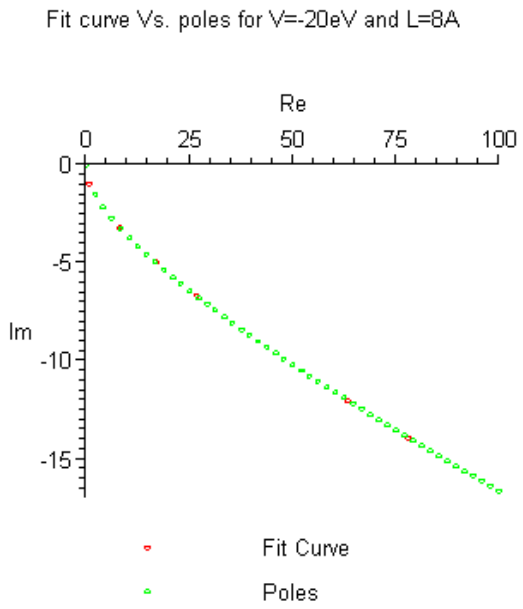

Figure 17-the fit curve superimposed on the poles for a square-well potential V=-20eV and L=8A.

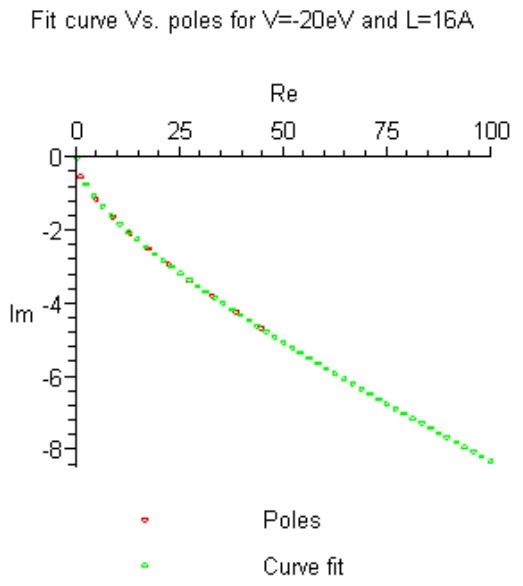

Figure 18-the fit curve superimposed on the poles for a square-well potential V=-20eV and L=16A.

The actual expression for the fitted curve in Figure 17 is

$$-0.07661407818728931 12z - 0.898464827048214620\sqrt{z}$$

and the fitted curve in Figure 18 is

$$-0.039510378285747993 4z - 0.435523411973303854\sqrt{z}$$

The constants a and b vary as the depth or width increase and this is obvious but how do they? In order to properly analyze how the constants depend on the depth and width, many data sets were studied, a total of 25 to be precise. Included in each data set were 8 or 9 poles corresponding to the energy with a real and imaginary part. A fitted curve or

mathematical expression was generated from each data set. Below shows two tables, one with coefficient a and the other with coefficient b.

Coefficient a	δ=8A	δ=12A	δ=16A	δ=20A	δ=24A
V=-20eV	- 0.076614	- 0.052208	- 0.039510	- 0.032052	- 0.026714
V=-25eV	- 0.070003	- 0.046362	- 0.034683	- 0.028547	- 0.023905
V=-35eV	- 0.059367	- 0.038772	- 0.027964	- 0.023780	- 0.019754
V=-60eV	- 0.045769	- 0.029007	- 0.020391	- 0.016631	- 0.014064
V=-100eV	- 0.034683	- 0.020751	- 0.014856	- 0.011507	- 0.009562

Table 2 – Coefficient a as it is varied with depth and width

Coefficient b	δ=8A	δ=12A	δ=16A	δ=20A	δ=24A
V=-20eV	- 0.898464	- 0.585560	- 0.435523	- 0.345094	- 0.287316
V=-25eV	- 0.884981	- 0.585908	- 0.437522	- 0.345956	- 0.287385
V=-35eV	- 0.879816	- 0.586420	- 0.443558	- 0.347699	- 0.290087
V=-60eV	- 0.870704	- 0.588049	- 0.447705	- 0.356187	- 0.295877
V=-100eV	- 0.875044	- 0.599412	- 0.452808	- 0.364246	- 0.303443

Table 3 – Coefficient b as it is varied with depth and width

Coefficient a looks to be affected by both the width and the depth of the potential; however coefficient b seems affected by the change in width but not so much the depth. Now, an explicit expression correlating the terms a and b with δ and V is created. First, the coefficients were paired up with its width counterpart, the width being the dependent variable, and data sets were created and plotted. Both the coefficients behaved as -1/ δ for each of the data sets. As an example, the depth V=-20eV for coefficient a is plotted as the width is varied below.

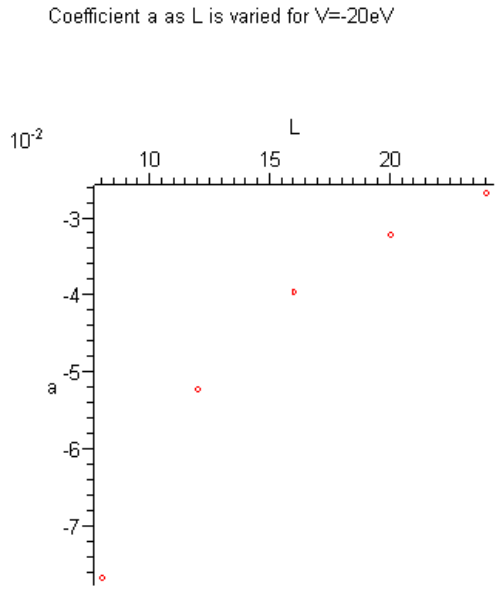

Figure 19-coefficient a vs. width for V=-20eV

The exact curve for each of the data sets is shown below (notation L=δ=width)

For coefficient a	Curve
V=-20eV	-0.622321738/L
V=-25eV	-0.560213818/L
V=-35eV	-0.469261721/L
V=-60eV	-0.352650898/L
V=-100eV	-0.259411531/L

Table 4- Mathematical expression for coefficient a as a function of the width L.

For coefficient b	Curve
V=-20eV	-7.083637782/L
V=-25eV	-7.035265689/L
V=-35eV	-7.034421631/L
V=-60eV	-7.031867201/L
V=-100eV	-7.114136837/L

Table 5- Mathematical expression for coefficient b as a function of the width L.

There is now a new coefficient and it varies with the depth. In order to determine exactly how it varies, new data sets were created. One data set was created from table 4 and the other from table 5. The figures below show how each data set varies with the depth.

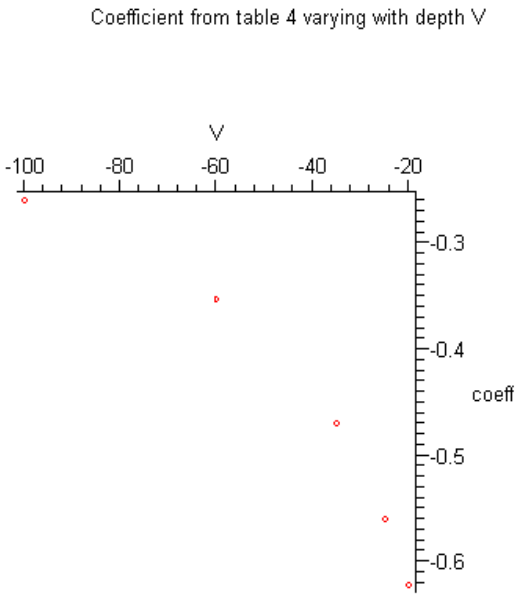

Figure 20 - coefficients from table 4 varying as the depth is increased.

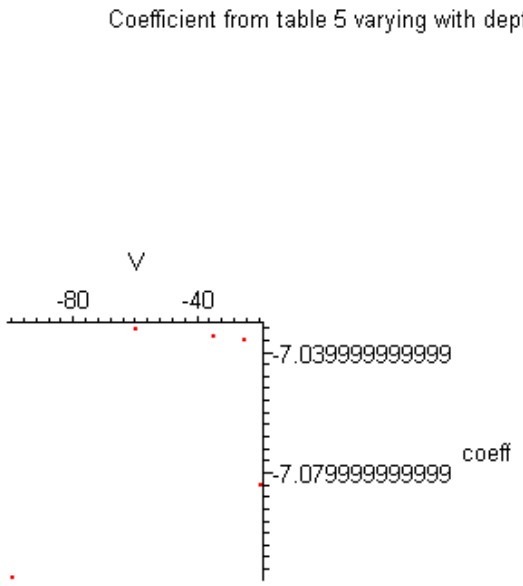

Figure 21 - coefficients from table 5 varying as the depth is increased.

Looking at figure 20, shows a curve that has an expression describing it explicitly 6.386817/V – 0.0014083*V-0.334848. Figure 21 isn't so simple since there is an outlying point for V=-100eV, -7.114136837. Since the terms don't vary that much with V, the outlying point at V=-100eV was disregarded. The expression that describes the curve now is -7.033736727 - 2.421415435 x 10^7 *e^V. This expression is a bit "ugly" but it does describe curve quite accurately. Finally, we have an expression in terms of the parameters, V and δ. The pole trajectory expression is

$$\frac{\left(-0.3348 - 0.001408\,V + \frac{6.386817}{V}\right)E}{L} + \frac{\left(-7.033736727 - 2.42141543510^{7}\,e^{V}\right)\sqrt{E}}{L}$$

This expression proves to be a very good approximation for any square well potential within the parameters used to create this trajectory (8<L<24 and -100<V<-20). If the parameters of the square well are outside these limits, the fitted curve starts to deviate from the actual poles as indicated in Figure 25. The figures below show the fit curve superimposed upon the poles for various parameters.

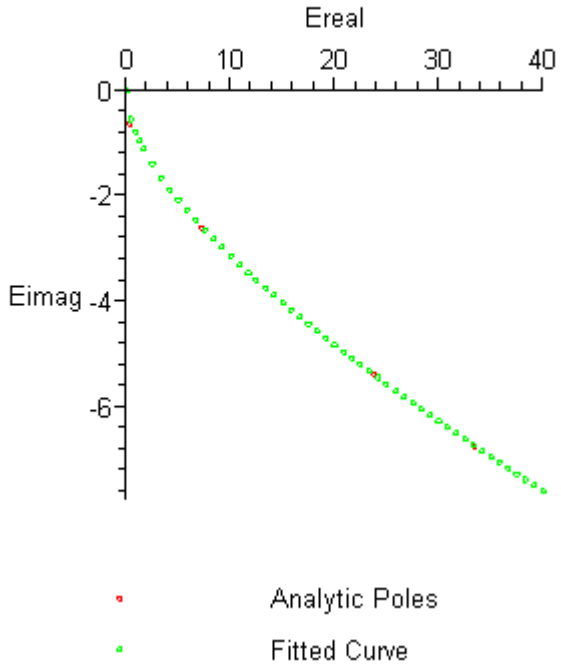

Figure 22- Pole trajectory fitted curve Vs. Analytic Poles for V=-22eV, L=9

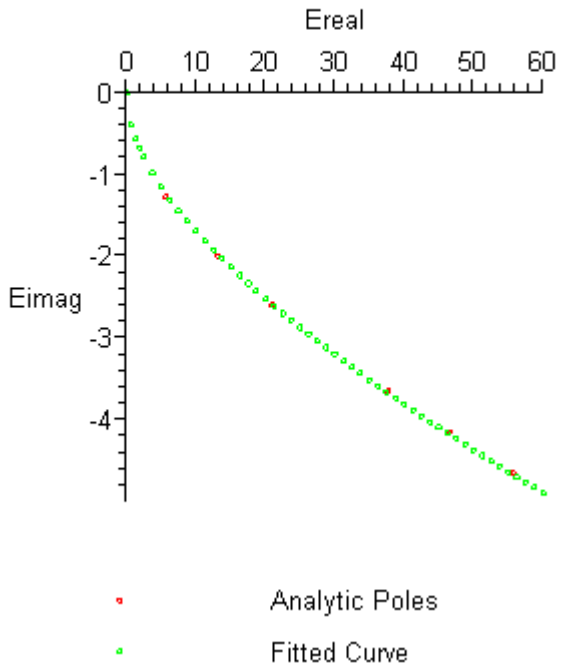

Figure 23- Pole trajectory fitted curve Vs. Analytic Poles for V=-75eV, L=15

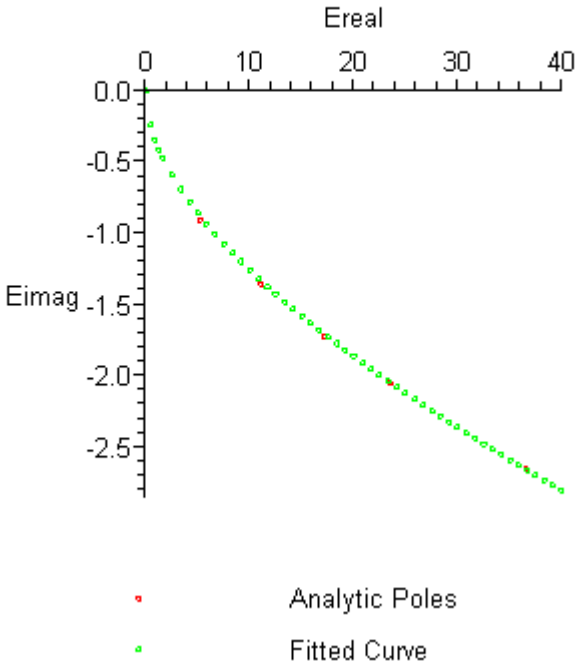

Figure 24- Pole trajectory fitted curve Vs. Analytic Poles for V=-85eV, L=20

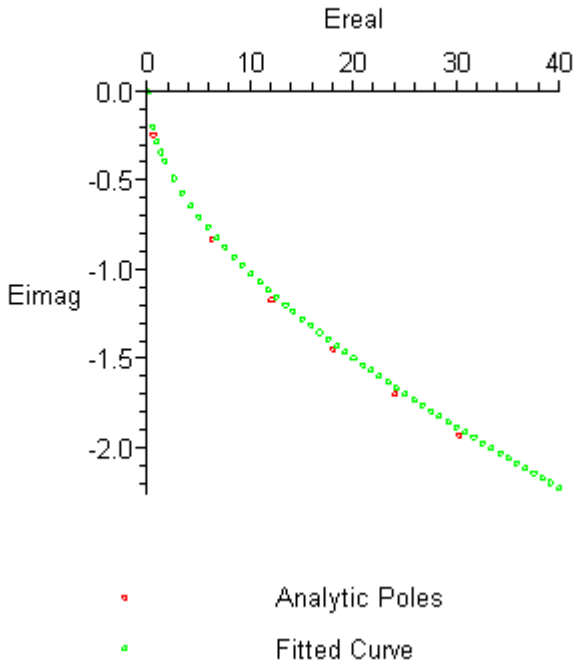

Figure 25- Pole trajectory fitted curve Vs. Analytic Poles for V=-120eV, L=24

Now that an accurate analytic expression has been found for the square-well potential in predicting the pole trajectory, it is only nature to find a similar expression to the piecewise approximation to a Gaussian potential. Referring the reader to figures 11 and 12 show that the transmission probability for this potential vary from 0.98 to 1.00 after 2eV. Since most of the structure has been washed out and that the transmission probability is $|1/T_{11}|^2$, we can assume that as we look for poles the matrix element T_{11} will be very similar for most energy. Also note that the element T_{11} is not analytic for this potential but numeric. Code was developed to find T_{11} with the results presented below for V_0=-20eV and L=8A.

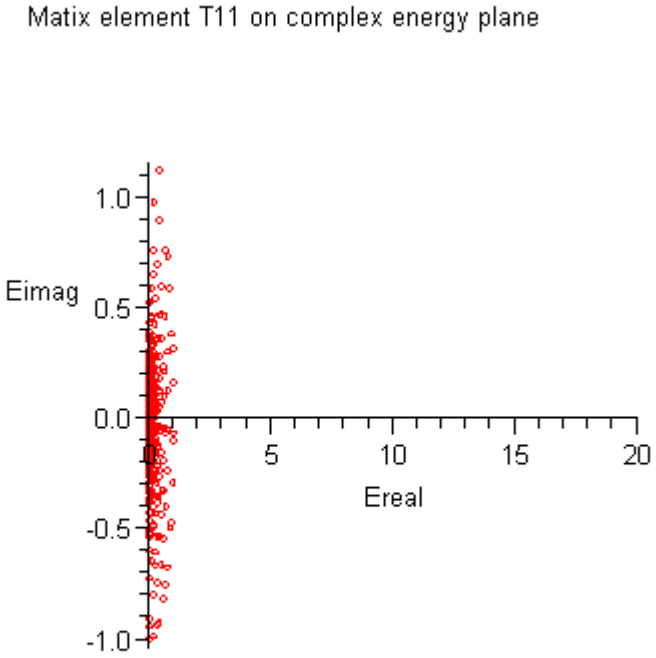

Figure 26 – Matrix element T_{11} on complex energy plane

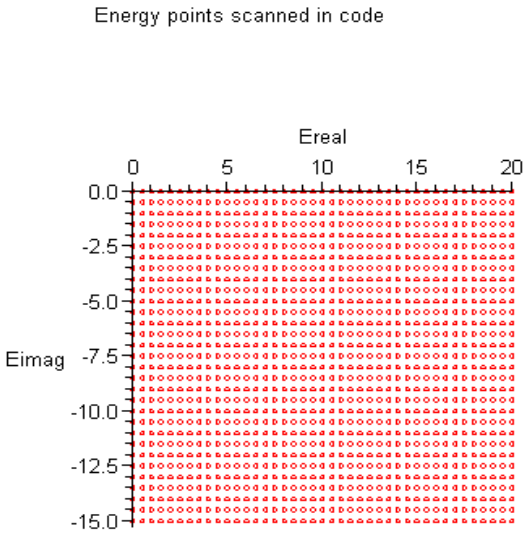

Figure 27 – the complex energy scanned in code

Realizing that energy has to be scanned for the complex grid at discrete points presented some difficulties. The obvious difficulty being that the "correct" energy that makes the element T_{11}=0, could have not have been selected. Also looking at figure 26, one sees that the elements all converge around 0+0*I! This makes it very difficult to determine which energy is "more correct". For example, if a certain energy makes the element T_{11}=0.00000456+0.00245*I and another makes the element T_{11}=0.000245+0.000056*I, both the elements look very close to 0+0*I but which one is "more correct". This is an issue that one must deal with when computing numerically. One might try to apply a filter to get the element as close to 0+0*I as possible. This was applied to the problem above with results;

```
> for j from -15 by 0.5 to 0 do
  for i from 0 by 0.5 to 20 do
  if (ℜ(T[j, i]) < 0.0004) then
  if (ℑ(T[j, i]) < 0.0004) then
  Test3[j, i] := Energy[j, i] :
  fi; fi; od; od;
```

```
Error, cannot determine if this expression is true or
false: 193.1601306*30^(1/2)+204.1749224*15^(1/2)*2^(1/2) <
2176.464516
```

It seems that some of the elements aren't all calculated numerically but left in an analytical state. This presents another problem because the filter doesn't know what to do as indicated in the error message above. Seeing all these problems just to get a few poles on one size of the Gaussian leads me to believe that this is a computer science problem and isn't tackled in this paper. The trajectory curve for the piece-wise Gaussian is assumed to be of the same structure as the square well potential based on the transmission resonance and bound states.

Relations between residues and poles

The S-Matrix can be expressed as the sum over simple poles

$$S(z) = \sum_i \frac{R(i)}{z - E(i)}$$

Z is a complex variable, E(i) are the complex poles of the S-Matrix for the potential investigated, and R(i) is the residue of the pole.[2] There exist non-trivial relations between the residues and the poles because the transmission probabilities max out at 1 for real energy z. Explicitly the transmission probability is

$$T(z) = \left| \sum_i \frac{R(i)}{z - E(i)} \right|^2$$

and this was shown previously. Even with the mathematical expression that was developed previously for the square well potential, the residues couldn't be found using Maple. Therefore for the reader to see that a relationship exists between the poles and residues, random values for the residues were selected. Then the transmission probability

that is generated from the function above is compared to figures 7, 8, 9, and 10. The reader will observe that the probability spectrum looks nothing like those figures.

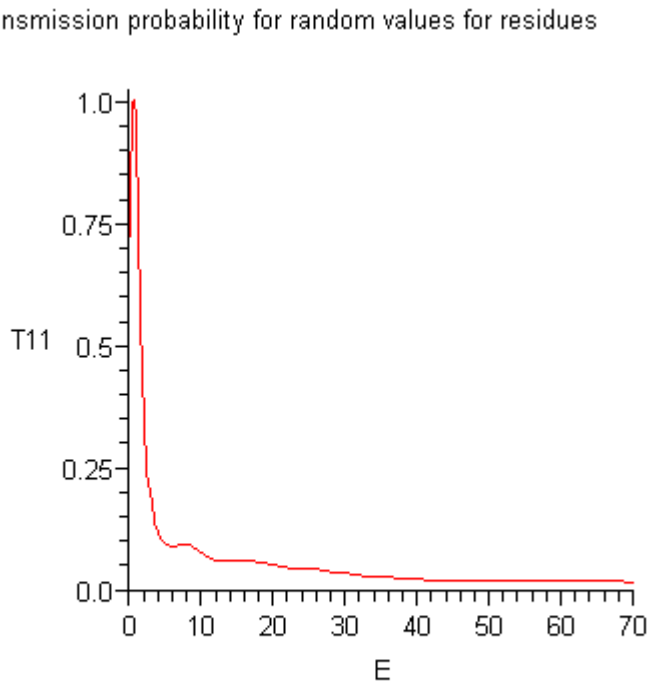

Figure 28 – Transmission probability for square well potential V=-20eV and L=8A using random residues

There were six bound states and the first eight poles were used to generate figure 28. One can see that this doesn't look anything like the transmission probability from figure 7. Therefore, there are some constraints on the residues and corresponding poles. They are related in someway or another, exactly how is a different story.

References

[1] Gilmore, Robert. *Elementary Quantum Mechanics in one Dimension,* Baltimore & London: John Hopkins, 2004.

[2] Gilmore, Robert.